# Ligand orientation governs conjugation capacity of UDP-glucuronosyltransferase 1A1

Takaoka, Yutaka ; Ohta, Mika ; Takeuchi, Atsuko ; Miura, Kenji ; Matsuo, Masafumi ; Sakaeda, Toshiyuki ; Sugano, Aki ; Nishio, Hisahide

(Citation)
Journal of biochemistry,148(1):25-28

(Issue Date)
2010-04-30

(Resource Type)
journal article

(Version)
Accepted Manuscript

(URL)
https://hdl.handle.net/20.500.14094/90001465

# Ligand orientation governs conjugation capacity of UDP-glucuronosyltransferase 1A1

Yutaka Takaoka[a, b], Mika Ohta[a, b], Atsuko Takeuchi[c], Kenji Miura[b], Masafumi Matsuo[a], Toshiyuki Sakaeda[d], Aki Sugano[a], Hisahide Nishio[e]

*[a]Division of Applied Genome Science and Bioinformatics, Kobe University Graduate School of Medicine, Kobe 650-0017, Japan; [b]Laboratory for Applied Genome Science and Bioinformatics, Clinical Genome Informatics Centre, Kobe University Graduate School of Medicine, Kobe 650-0017, Japan; [c]Kobe Pharmaceutical University, Kobe 658-8558, Japan; [d]Center for Integrative Education of Pharmacy Frontier (Frontier Education Center), Graduate School of Pharmaceutical Sciences, Kyoto University, Kyoto 606-8501; [e]Department of Genetic Epidemiology, Kobe University Graduate School of Medicine, Kobe 650-0017, Japan*

Running head: Ligand orientation governs conjugation capacity of UGT1A1

Address for reprint requests and other correspondence: Yutaka TAKAOKA, Division of Applied Genome Science and Bioinformatics, Kobe University Graduate School of Medicine, Kobe 650-0017, Japan
Tel: +81-78-382-5111 (Ext. 2765); Fax: +81-78-382-5839
*E-mail address:* ytakaoka@med.kobe-u.ac.jp

***Abbreviations*:** UGT1A1, UDP-glucuronosyltransferase 1A1; UDPGA, UDP-glucuronic acid; RMS, root mean square

**Abstract**

UDP-glucuronosyltransferase 1A1 (UGT1A1) is an endoplasmic reticulum membrane protein that catalyzes glucuronidation. Mutant UGT1A1 possesses a different conjugation capacity, and the molecular mechanisms regulating these conjugation reactions are as yet unclear. To elucidate these molecular mechanisms, we simulated and analyzed the glucuronidation of wild-type UGT1A1 and six UGT1A1 mutants, with bilirubin as the substrate. We found that only the orientation of the substrates correlated with the conjugation capacity in *in vitro* experiments. Inasmuch as glucuronidation is an intermolecular rearrangement reaction, we find that the conjugation reaction proceeds only when the hydroxyl group of the substrate is oriented toward the coenzyme, which allows the electron transfer to occur.

**Keywords**: Molecular modeling; Docking simulation; Conjugation capacity; Glucuronidation; Substrate orientation; UGT1A1

UDP-glucuronosyltransferases (UGTs) constitute a membrane-bound enzyme family whose members catalyze glucuronidation, which is an important process for the clearance of drugs, endogenous compounds, dietary chemicals, and environmental pollutants from the body. UGTs also facilitate excretion of the products of phase I metabolism. UGTs are classified into three subfamilies—UGT1A, UGT2A, and UGT2B—on the basis of sequence homology and gene structure. UGT1A1, one of the nine isoforms of the UGT1A subfamily, was generated by alternative splicing of exon 1 to the four common exons (exons 2–5) on chromosome 2q37 (1). UGT1A1 is the only enzyme involved in bilirubin glucuronidation (2), and numerous mutations of the UGT1A1 gene have been discovered in patients with Gilbert's syndrome and Crigler-Najjar syndrome, which are characterized by jaundice (1). Although *in vitro* analyses of the conjugation capacity of UGT1A1 mutants have been reported (3, 4, 5), the molecular mechanisms of this conjugation reaction are still unclear.

The 3D structure of human UGT1A1 was determined via homology modeling, by using a grape flavonoid glucosyltransferase (*Vitis vinifera* 3-*O*-glucosyltransferase, VvGT1), UGT71G1 from *Medicago truncatula*, and UGT2B7 from *homo sapiens* as the template (6, 7, 8). The X-ray crystallographic structures used as templates in these studies provided data including the binding of the coenzyme to the glycosyltransferases, specifically, the binding sites of UGT1A1 and coenzymes and the reactive sites of conjugation with substrates (9). Moreover, recent advances in high-performance computer technology have enabled practical applications of molecular simulation programs (10, 11, 12, 13, 14, 15) for protein analysis. In this study, we analyzed the molecular mechanisms of the conjugation reaction of UGT1A1 by using *in silico* simulations. The aim of this study was to elucidate, by means of both molecular simulation and *in vitro* experimental results, the molecular mechanisms of the conjugation reaction of UGT1A1 and the key factors involved in the reaction so as to define the conjugation capacity of UGT1A1.

We performed three molecular simulations for each glucuronidation step: docking of UGT1A1 with UDPGA, induced fit for the docking model of UGT1A1 with UDPGA, and docking to elucidate bilirubin orientation (Fig. 1). For docking models with a coenzyme, we similarly analyzed the orientation of bilirubin for each model structure and then calculated the average results of the number of simulations that had the hydroxyl group of bilirubin oriented toward UDPGA, which we named the hydroxyl orientation. We calculated the mean ± SD of docking energy for each UGT1A1 mutant with the hydroxyl orientation of bilirubin and the other orientations.

We compared our simulation results with the *in vitro* conjugation capacity of each mutant UGT1A1 as determined on the basis of three previous reports. Specifically, values for G71R, F83L, and I294T, as a percentage of the wild-type UGT1A1 value, were based on data from Yamamoto et al. (5), Udomuksorn et al. (4), and Ciotti et al. (3), respectively. We also calculated the values of bilirubin conjugation capacity, as a percentage of the wild-type value, for R336L, N400D, and W461R, which cause Crigler-Najjar syndrome type I or II (the classification of type I or II depends on the blood concentration of bilirubin).

As a result of comparison with the values for *in vitro* conjugation capacity, we found a good correlation only for the number of hydroxyl orientations of bilirubin (Fig. 2). The other results of our simulations—that is, the number of native orientations of UDPGA, the docking energy of UDPGA with UGT1A1, and the docking energy of bilirubin into UGT1A1—had no correlation with *in vitro* conjugation capacity. Table 1 shows a summary of our analysis of the molecular simulations. For both docking energy results, no significant differences between the orientations were observed. Our results therefore suggested that the conjugation capacity of UGT1A1 was controlled by the hydroxyl orientation of the substrate.

As shown in Figure 3, we propose that the hydroxyl orientations of bilirubin governs the

conjugation capacity for glucuronidation, with the mechanism based on the hypothetical mechanism of glycoconjugation achieved by the glycosyltransferase (16, 17). During glucuronidation with bilirubin in the hydroxyl orientation, the hydroxyl group is deprotonated by the acidic amino acid of UGT1A1, and the resultant oxygen atom of bilirubin and the glycosyl group of UDPGA undergo a nucleophilic reaction, which produces bilirubin glucuronide. The oxygen at the cleavage site of glucuronic acid of UDPGA is then protonated by $NH_2$ (the amino group) of a basic amino acid (Fig. 3B). During glucuronidation with bilirubin in another orientation, its hydroxyl group cannot be deprotonated because it does not point toward the acidic amino acid of UGT1A1, and no side chain for deprotonation exists (Fig. 3C). We therefore concluded that this specific molecular mechanism governs UGT1A1 conjugation capacity.

In this paper, we present a new model for a molecular mechanism of bilirubin glucuronidation by UGT1A1. Substrate orientation is a key factor in the glucuronidation reaction of UGT1A1 with bilirubin, as well as with substrates other than bilirubin (18). Indeed, our experimental results of the simulation for SN-38 indicated a correlation between substrate orientation and *in vitro* conjugation capacity: comparison among Wild, G71R, P229Q and L233R showed that 100%, 49%, 9%, 11% for *in vitro* conjugation capacity (19) and 66, 30, 17, 19 for hydroxyl orientations in 100 simulations, respectively. In addition, 17β-estradiol undergoes glucuronidation at only the one-tailed hydroxyl group (the 3-OH on the A ring) (20). These results suggest that the conjugation capacity of UGT1A1 is mainly controlled by substrate orientation. In addition, our simulation findings did not depend on the particular simulation program, because we confirmed the correlation between substrate orientation and *in vitro* conjugation capacity by also using the MOE program (data not shown).

We therefore propose a molecular mechanism of conjugation capacity that is governed by

substrate orientation, as analogous to reaction mechanisms of glycoconjugates in the glycosyltransferase reaction (17). This proposed mechanism of glucuronidation (Fig. 3) suggests that the hydroxyl group of the substrate is required for the transfer reaction of glucuronic acid to occur.

Mutant UGT1A1 is known to cause not only hyperbilirubinemia but also adverse effects of chemotherapy (21). Indeed, patients in the United States and Japan are encouraged to undergo a genetic test for UGT1A1 before beginning chemotherapy (22). Being able to predict *in silico* conjugation capacity of UGT1A1 is important because more than 70 mutants have already been reported, with other mutations expected to be found in the future. We believe that these molecular simulation results, primarily related to substrate orientation, may lead to prediction of the conjugation capacity of other UGT1A1 mutants.

**Supplementary Data**

Supplementary Data are available at JB Online.

**Acknowledgements**

We thank Professor Takashi Iyanagi (SPring8, Japan) for his helpful comments. This study was supported, in part, by a grant-in-aid for Cancer Research of the Hyogo Prefecture Health Promotion Association; Research grant from the YOKOYAMA Foundation for Clinical Pharmacology and Therapeutics; and a grant-in-aid for Scientific Research from the Ministry of Science, Culture and Sports, Japan.

**References**


1. Owens, I.S., Basu, N.K., and Banerjee, R. (2005) UDP-glucuronosyltransferases: gene structures of UGT1 and UGT2 families. *Methods Enzymol.* **400**, 1-22

2. Marsh, S., McKay, J.A., Cassidy, J., and McLeod, H.L. (2001) Polymorphism in the thymidylate synthase promoter enhancer region in colorectal cancer. *Int. J. Oncol.* **19**, 383-386

3. Ciotti, M., Chen, F., Rubaltelli, F.F., and Owens, I.S. (1998) Coding defect and a TATA box mutation at the bilirubin UDP-glucuronosyltransferase gene cause Crigler-Najjar type I disease. *Biochim. Biophys. Acta* **1407**, 40-50

4. Udomuksorn, W., Elliot, D.J., Lewis, B.C., Mackenzie, P.I., Yoovathaworn, K., and Miners, J.O. (2007) Influence of mutations associated with Gilbert and Crigler-Najjar type II syndromes on the glucuronidation kinetics of bilirubin and other UDP-glucuronosyltransferase 1A substrates. *Pharmacogenet. Genomics* **17**, 1017-1029

5. Yamamoto, K., Sato, H., Fujiyama, Y., Doida, Y., and Bamba, T. (1998) Contribution of two missense mutations (G71R and Y486D) of the bilirubin UDP glycosyltransferase (UGT1A1) gene to phenotypes of Gilbert's syndrome and Crigler-Najjar syndrome type II. *Biochim. Biophys. Acta* **1406**, 267-273

6. Offen, W., Martinez-Fleites, C., Yang, M., Kiat-Lim, E., Davis, B.G., Tarling, C.A., Ford, C.M., Bowles, D.J., and Davies, G.J. (2006) Structure of a flavonoid glucosyltransferase reveals the basis for plant natural product modification. *EMBO J.* **25**, 1396-1405

7. Shao, H., He, X., Achnine, L., Blount, J.W., Dixon, R.A., and Wang, X. (2005) Crystal structures of multifunctional triterpene/flavonoid glycosyltransferase from Medicago truncatula. *The Plant Cell* **17**, 3141-3154

8. Laakkonen, L. and Finel, M. (2010) A molecular model of the human UGT1A1, its membrane orientation and the interactions between different parts of the enzyme. *Mol Pharmacol* doi:10.1124/mol.109.063289

9. Radominska-Pandya, A., Bratton, S.M., Redinbo, M.R., and Miley, M.J. (2010) The crystal structure of human UDP-glucuronosyltransferase 2B7 C-terminal end is the first mammalian UGT target to be revealed: the significance for human UGTs from both the 1A and 2B families. *Drug Metab Rev* **42**, 128-39

10. Molecular Operating Environment (MOE) Version 2009.10. Chemical Computing Group Inc., Montreal, Quebec, Canada, http://www.chemcomp.com/software-moe2009.htm (Accessed on April 22, 2010)

11. DeLano, W.L. (2002) The PyMOL molecular graphics system. DeLano Scientific, Palo alto, CA, USA, http://www.pymol.org/ (Accessed on April 22, 2010)

12. Guex, N. and Peitsch, M.C. (1997) SWISS-MODEL and the Swiss-PdbViewer: An environment for comparative protein modeling. *Electrophoresis* **18**, 2714-2723

13. Morris, G.M., Goodsell, D.S., Halliday, R.S., Huey, R., Hart, W.E., Belew, R.K., and Olson, A.J. (1998) Automated docking using a Lamarckian genetic algorithm and an empirical binding free energy function. *J. Comput. Chem.* **19**, 1639-1662

14. Ren, P. and Ponder, J.W. (2003) Polarizable atomic multipole water model for molecular mechanics simulation. *J. Phys. Chem. B.* **107**, 5933-5947

15. Fujiwara, R., Nakajima, M., Yamamoto, T., Nagao, H., and Yokoi, T. (2009) In silico

and in vitro approaches to elucidate the thermal stability of human UDP-glucuronosyltransferase (UGT) 1A9. *Drug Metab Pharmacokinet* **24**, 235-44

16. Davies, G.J., Mackenzie, L., Varrot, A., Dauter, M., Brzozowski, A.M., Schülein, M., and Withers, S.G. (1998) Snapshots along an enzymatic reaction coordinate: analysis of a retaining β-glycerincoside hydrolase. *Biochemistry* **37**, 11707-11713
17. Kapitonov, D. and Yu, R.K. (1999) Conserved domains of glycosyltransferases. *Glycobiology* **9**, 961-978
18. Kiang, T.K.L., Ensom, M.H.H., and Chang, T.K.H. (2005) UDP-glucuronosyltransferases and clinical drug-drug interactions. *Pharmacol. & Ther.* **106**, 97-132
19. Gagne, J.F., Montminy, V., Belanger, P., Journault, K., Gaucher, G., and Guillemette, C. (2002) Common human UGT1A polymorphisms and the altered metabolism of irinotecan active metabolite 7-ethyl-10-hydroxycamptothecin (SN-38). *Mol Pharmacol* **62**, 608-17
20. Itäaho, K., Mackenzie, P.I., Ikushiro, S., Miners, J.O., and Finel, M. (2008) The configuration of the 17-hydroxy group variably influences the glucuronidation of β-estradiol and epiestradiol by human UDP-glucuronosyltransferase. *Drug Metab. Dispos.* **36**, 2307-2315
21. Ando, Y., Saka, H., Ando, M., Sawa, T., Muro, K., Ueoka, H., Yokoyama, A., Saitoh, S., Shimokata, K., and Hasegawa, Y. (2000) Polymorphisms of UDP-glucuronosyltransferase gene and irinotecan toxicity: a pharmacogenetic analysis. *Cancer Res.* **60**, 6921-6926
22. Gold, H.T., Hall, M.J., Blinder, V., and Schackman, B.R. (2009) Cost effectiveness of

pharmacogenetic testing for uridine diphosphate glucuronosyltransferase 1A1 before irinotecan administration for metastatic colorectal cancer. *Cancer* **115**, 3858-3867

**Figure Legends**

**Fig. 1.** Schematic drawing of the glucuronidation-based molecular simulation for conjugation of bilirubin and UDPGA. Boxes provide details of the molecular simulation process.

**Fig. 2.** Orientation of the bilirubin to UDPGA (i.e., number of orientations in which the hydroxyl group of bilirubin points toward UDPGA) (A) and the in vitro conjugation capacity (B), as related to wild-type UGT1A1 and UGT1A1 mutants.

**Fig. 3.** The mechanism of bilirubin glucuronidation by means of the conjugation reaction of UGT1A1. The bilirubin molecule has two dipyrrole moieties (referred to as R and R') with two hydroxyl groups (A). With bilirubin in the hydroxyl orientation, glucuronidation of bilirubin with glucuronic acid occurs in three steps: (1) deprotonation of the hydroxyl group, (2) nucleophilic reaction with UDPGA, and (3) protonation of UDP (B). With bilirubin in another orientation, this glucuronidation mechanism cannot operate (C).

**Table 1.** Results of molecular simulations of bilirubin conjugation with wild-type UGT1A1 and UGT1A1 mutants

| Measure | Orientation | Wild type | G71R | F83L | I294T | R336L | N400D | W461R |
|---|---|---|---|---|---|---|---|---|
| No. of native orientations of UDPGA (50 simulations) | | 12 | 12 | 11 | 10 | 18 | 15 | 10 |
| Docking energy of UGT1A1 and UDPGA (kcal/mol) | Reactive | −3.81 ± 1.48 | −4.15 ± 1.15 | −2.28 ± 0.58 | −2.97 ± 1.92 | −3.42 ± 2.08 | −2.36 ± 1.18 | −1.98 ± 3.06 |
| | Other | −3.82 ± 1.39 | −3.48 ± 1.18 | −2.93 ± 1.11 | −2.59 ± 2.81 | −2.25 ± 2.32 | −1.70 ± 2.38 | −2.37 ± 1.60 |
| No. of hydroxyl orientations of bilirubin (300 simulations) | | 91 | 46 | 34 | 59 | 88 | 58 | 42 |
| Docking energy of UGT1A1 and bilirubin (kcal/mol) | Hydroxyl | −7.15 ± 0.95 | −7.16 ± 3.17 | −6.79 ± 1.32 | −8.01 ± 1.09 | −7.19 ± 1.05 | −6.83 ± 1.23 | −7.63 ± 1.11 |
| | Other | −7.53 ± 0.90 | −7.17 ± 3.24 | −8.49 ± 1.36 | −7.87 ± 1.15 | −7.12 ± 1.15 | −7.09 ± 1.17 | −7.62 ± 1.03 |

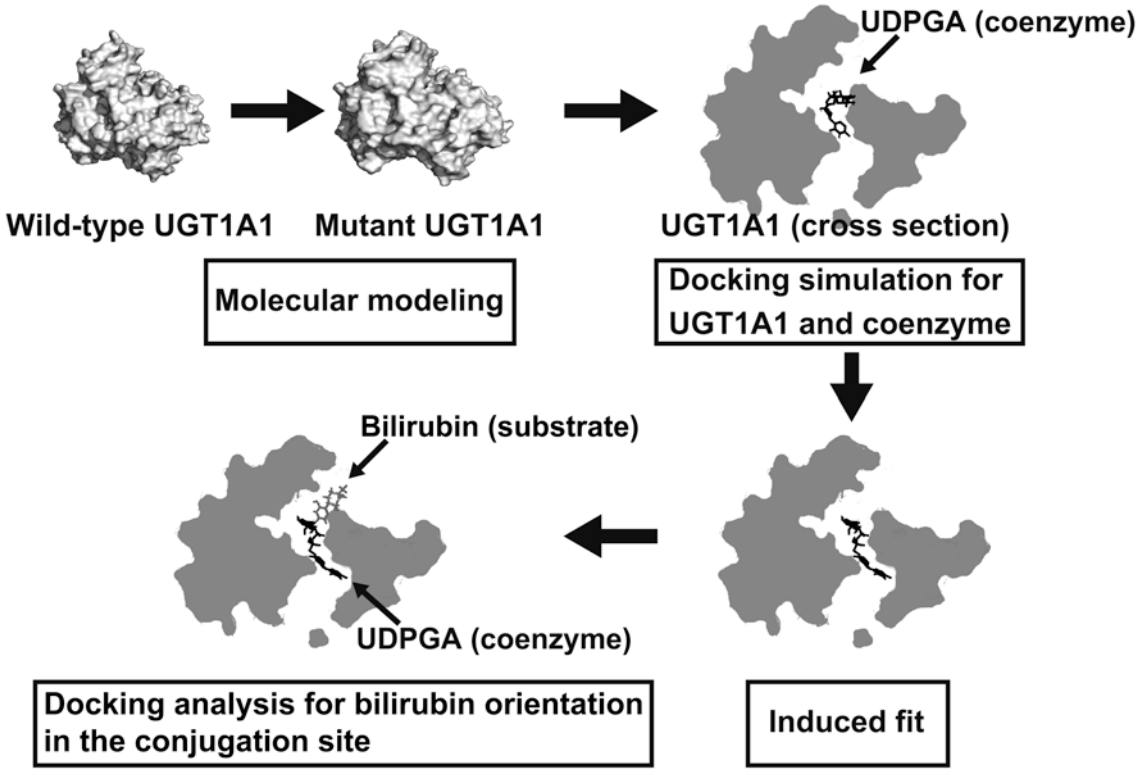
UDPGA (coenzyme)
Wild-type UGT1A1
Mutant UGT1A1
UGT1A1 (cross section)
Molecular modeling
Docking simulation for UGT1A1 and coenzyme
Bilirubin (substrate)
UDPGA (coenzyme)
Docking analysis for bilirubin orientation in the conjugation site
Induced fit

Fig.1

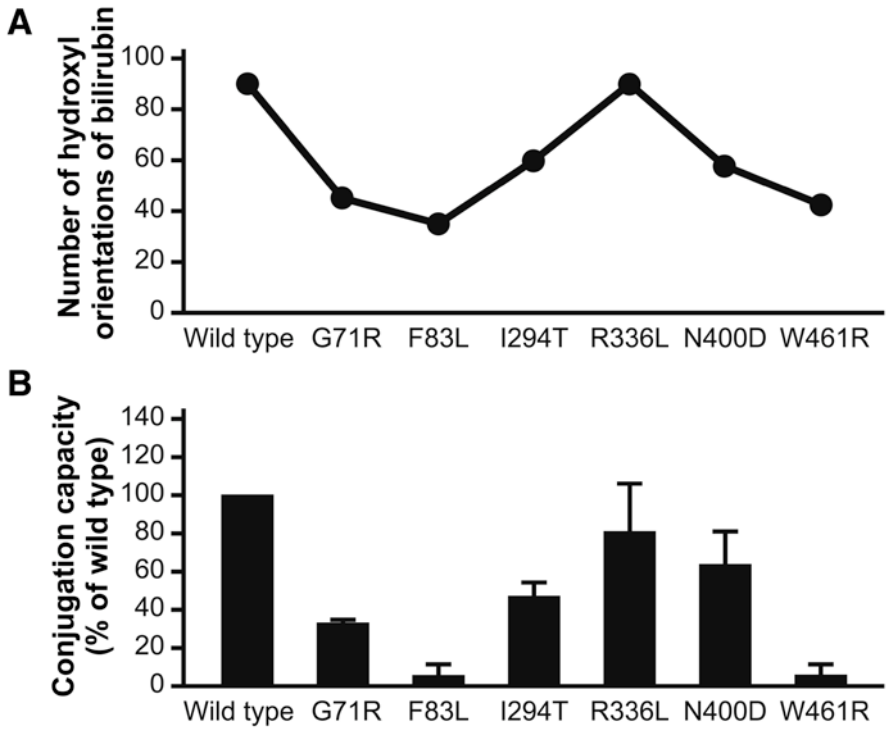
A
Number of hydroxyl orientations of bilirubin
100
80
60
40
20
0
Wild type
G71R
F83L
I294T
R336L
N400D
W461R
B
Conjugation capacity (% of wild type)
140
120
100
80
60
40
20
0
Wild type
G71R
F83L
I294T
R336L
N400D
W461R

Fig. 2

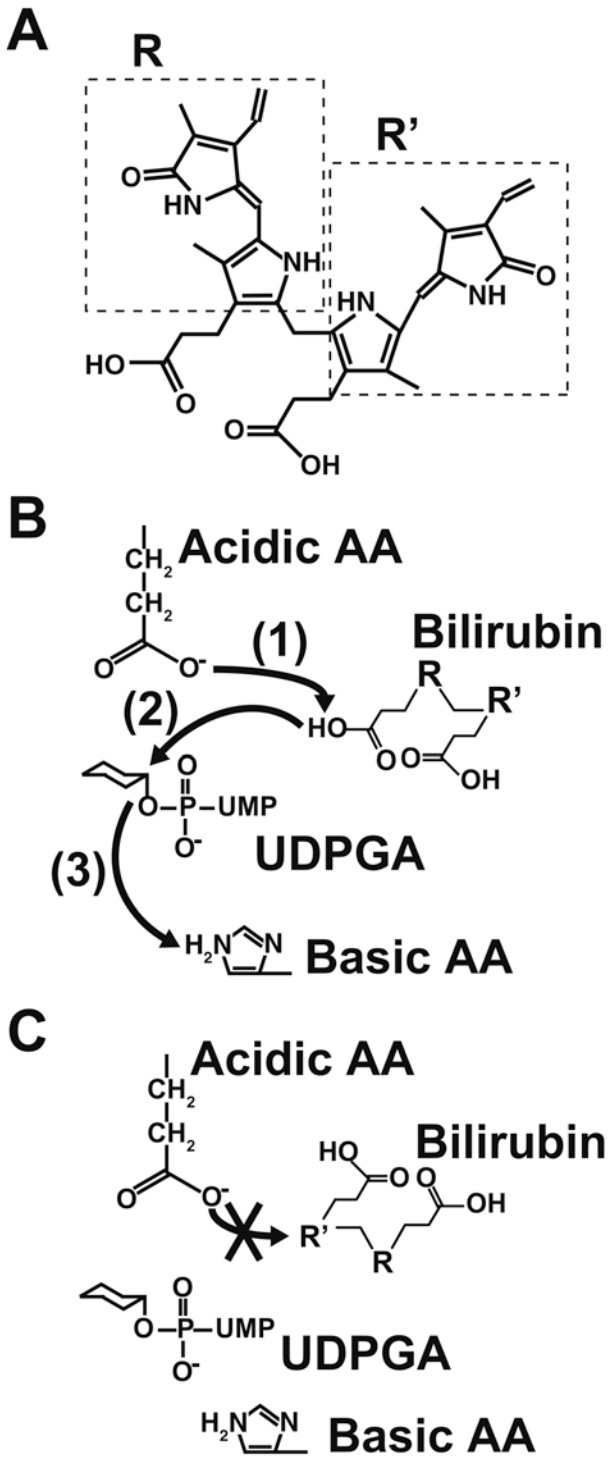
A
R
R'
B
Acidic AA
Bilirubin
(1)
(2)
(3)
UDPGA
Basic AA
C
Acidic AA
Bilirubin
UDPGA
Basic AA

Fig. 3

# Supporting materials

for

# Ligand orientation governs conjugation capacity of UDP-glucuronosyltransferase 1A1

Yutaka Takaoka, Mika Ohta, Atsuko Takeuchi, Kenji Miura, Masafumi Matsuo, Toshiyuki Sakaeda, Aki Sugano, Hisahide Nishio

## Supplementary Methods and Results

### *Molecular simulation of UGT1A1 glucuronidation*

The 3D structure of UGT1A1 was downloaded from the ModBase database (1) (database ID: gi 8850236). After we added hydrogen atoms to the model structure via PyMOL software (2), we prepared structures of UGT1A1 mutants (G71R, F83L, I294T, R336L, N400D, and W461R) by using Swiss-PdbViewer (3). The structural data were then subjected to energy minimization by means of the MINIMIZE program of the TINKER package (4) with the AMBER99 force field. Minimization was performed until the root mean square (RMS) gradient was 0.3 kcal/mol/Å. We used the AutoDock 4 program (5) for simulation of UDPGA docking with each UGT1A1 mutant. The 3D structure of UDPGA was downloaded from ChemIDplus (registry number: 2616-64-0). We used all of the five available structures for the docking simulation with each UGT1A1. The ligand-centered maps were generated by the program AutoGrid with a spacing of 0.375 Å and grid dimensions of 60 × 60 × 60 points. Grid searching was performed by using the Lamarckian genetic algorithm. All other parameters were defined by default settings. Ten different docking runs were performed for each UGT1A1-UDPGA pair (i.e., a total of 50 runs for each UGT1A1). After the docking simulation, we classified orientations of UDPGA on the basis of whether they could function in the conjugation reaction, and we calculated an average binding energy for each group of

orientations. The minimum sum-of-squares clustering, selected by the group average method, was used for binding models of UDPGA with each UGT1A1 mutant. We analyzed the number of occurrences of reactive orientations of UDPGA by using the binding models provided by previous reports. We then optimized these binding models by means of the induced-fit method of the MOE (Molecular Operating Environment) program (6); we used the AMBER99 force field until the RMS gradient was less than 0.3 kcal/mol/Å.

After we used the induced-fit method, we simulated bilirubin docking to each UGT1A1 mutant. The 3D structural data of bilirubin were downloaded from ChemIDplus (registry number: RN: 635-65-4). To investigate substrate orientations at the site determined by the docking model, we divided the site in which the substrate could be present during the conjugation reaction into three areas and analyzed the orientations of the substrates in each area. The ligand-centered map was generated by the AutoGrid program with a spacing of 0.375 Å and grid dimensions of 36 × 32 × 60, 50 × 39 × 30, and 36 × 47 × 30 points. One hundred different docking runs were performed for each of these three grids.

***In vitro conjugation capacity of UGT1A1 mutants with bilirubin***

We used values of the *in vitro* conjugation capacity for G71R, F83L, and I294T, which were reported as a percentage of the wild type. In addition to the values for these three mutations, we calculated the conjugation capacity of R336L, N400D, and W461R as a percentage of that of the wild type. The value for R336L was 81.6 ± 24.4%; that for N400D was 63.5 ± 18.1%, derived on the basis of the maximal range (30.6-55%) of the conjugation capacity from *in vitro* data for the two mutations in Crigler-Najjar syndrome type II, G71R and I295T; and that for W461R was 5 ± 5%, which was based on the value for F83L because both mutations cause Crigler-Najjar syndrome type I. Calculation procedures for these UGT1A1 mutants follow.

R336L was found in a heterozygous patient with Crigler-Najjar syndrome type II who carried a homozygous $(TA)_7$ mutation in the UGT1A1 promoter region (7). The bilirubin conjugation capacity influenced solely by the homozygous $(TA)_7$ mutation can be set to 51.7% of the wild type by applying the data for UGT1A1*28 reported by Peters et al. (8). In addition, the bilirubin conjugation capacity in patients with Crigler-Najjar syndrome type II is within 30.6-55% of that of the wild type according to previous reports (9, 10). The conjugation capacity of R336L was thus calculated by using the following equation:

$$30.6 < 100 - x/2 - 48 < 55$$

where $x$ is the reduction rate, compared with wild type, for the conjugation capacity of the R336L mutation.

N400D in the homozygous state causes Crigler-Najjar syndrome type II with the homozygous $(TA)_8$ mutation (11). G71R and I294T are the mutations found in patients with this disease. We used the *in vitro* conjugation capacity of these mutations, both in the homozygous state, as a percentage of the wild type: that for G71R was 30.6-33.8% (10) and that for I294T was 40-55% (9). In addition, the $(TA)_8$ mutation cause 67.4 % conjugation capacity of wild type (12).

W461R in the homozygous state was identified in a patient with Crigler-Najjar syndrome type I (13). The bilirubin conjugation capacity of this mutation was set to 0-10% of that of the wild type on the basis of a previous report for F83L (14), which was also found in a patient with Crigler-Najjar syndrome type I.

## References

1. Pieper, U., Eswar, N., Webb, B.M., Eramian, D., Kelly, L., Baikan, D.T., Carter, H., Mankoo, P., Karchin, R., Marti-Renom, M.A., Davis, F.P., and Sali, A. (2008) MODBASE, a database of annotated comparative protein structure models and associated resources. *Nucleic Acids Res.* **1**, 1-8

2. DeLano, W.L. (2002) The PyMOL molecular graphics system. DeLano Scientific, Palo alto, CA, USA
3. Guex, N. and Peitsch, M.C. (1997) SWISS-MODEL and the Swiss-PdbViewer: An environment for comparative protein modeling. *Electrophoresis* **18**, 2714-2723
4. Ren, P. and Ponder, J.W. (2003) Polarizable atomic multipole water model for molecular mechanics simulation. *J. Phys. Chem. B.* **107**, 5933-5947
5. Morris, G.M., Goodsell, D.S., Halliday, R.S., Huey, R., Hart, W.E., Belew, R.K., and Olson, A.J. (1998) Automated docking using a Lamarckian genetic algorithm and an empirical binding free energy function. *J. Comput. Chem.* **19**, 1639-1662
6. Molecular Operating Environment (MOE) Version 2009.10. Chemical Computing Group Inc., Montreal, Quebec, Canada
7. Servedio, V., d'Apolito, M., Maiorano, N., Minuti, B., Torricelli, F., Ronchi, F., Zancan, L., Perrotta, S., Vajro, P., Boschetto, L., and Iolascon, A. (2005) Spectrum of UGT1A1 mutations in Crigler-Najjar (CN) syndrome patients: identification of twelve novel alleles and genotype-phenotype correlation. *Hum. Mutat.* **25**, 325
8. Peters, W.H.M., te Morsche, R.H., and Roelofs, H.M. (2003) Combined polymorphisms in UDP-glucuronosyltransferases 1A1 and 1A6: implications for patients with Gilbert's syndrome. *J. Hepatol.* **38**, 3-8
9. Ciotti, M., Chen, F., Rubaltelli, F.F., and Owens, I.S. (1998) Coding defect and a TATA box mutation at the bilirubin UDP-glucuronosyltransferase gene cause Crigler-Najjar type I disease. *Biochim. Biophys. Acta* **1407**, 40-50
10. Yamamoto, K., Sato, H., Fujiyama, Y., Doida, Y., and Bamba, T. (1998) Contribution of two missense mutations (G71R and Y486D) of the bilirubin UDP glycosyltransferase (UGT1A1) gene to phenotypes of Gilbert's syndrome and Crigler-Najjar syndrome type II. *Biochim. Biophys. Acta* **1406**, 267-273
11. Labrune, P., Myara, A., Chalas, J., Le Bihan, B., Capel, L., and Francoual, J. (2002) Association of a homozygous $(TA)_8$ promoter polymorphism and a N400D mutation of UGT1A1 in a child with Crigler-Najjar type II syndrome. *Hum. Mutat.* **20**, 399-401
12. Beutler, E., Gelbart, T., and Demina, A. (1998) Racial variability in the UDP-glucuronosyltransferase 1 (UGT1A1) promoter: a balanced polymorphism for regulation of bilirubin metabolism? *Proc. Natl. Acad. Sci. U. S. A.* **95**, 8170-8174
13. Maruo, Y., Nishizawa, K., Sato, H., Doida, Y., and Shimada, M. (1999) Association of neonatal hyperbilirubinemia with bilirubin UDP-glucuronosyltransferase polymorphism. *Pediatrics* **103**, 1224-1227
14. Udomuksorn, W., Elliot, D.J., Lewis, B.C., Mackenzie, P.I., Yoovathaworn, K., and

Miners, J.O. (2007) Influence of mutations associated with Gilbert and Crigler-Najjar type II syndromes on the glucuronidation kinetics of bilirubin and other UDP-glucuronosyltransferase 1A substrates. *Pharmacogenet. Genomics* **17**, 1017-1029